Carboxy Ester Hydrolysis Promoted by a Zinc(II) 2-[Bis(2-aminoethyl)amino]ethanol Complex: A New Model for Indirect Activation on the Serine Nucleophile by Zinc(II) in Zinc Enzymes

Jiang Xia,[†] Yan Xu,[†] Shu-an Li,[†] Wei-yin Sun,[†] Kai-bei Yu,[‡] and Wen-xia Tang*[,†]

State Key Laboratory of Coordination Chemistry, Nanjing University, Nanjing 210093, P.R. China, and Analysis Center, Chengdu Branch of the Chinese Academy of Sciences, Chengdu 610041, P.R. China

Received June 15, 2000

A complexation study on the new Zn(II) complexes of asymmetric tripodal ligand 2-[bis(2-aminoethyl)amino]-ethanol (L) has revealed that the alcoholic OH group of complex ZnL exhibits remarkable acidity with a very low pK_a value of 7.7 at 25 °C. Both the monomeric complex $[ZnH_{-0.25}L(H_2O)](ClO_4)_{1.75}$ (**I**) and the dimeric alkoxide-coordinating complex $[Zn_2(H_{-1}L)_2](ClO_4)_2$ (**II**) were synthesized, and their structures were determined by X-ray diffraction. The Zn(II)-bound alkoxide, as the reactive nucleopile toward the hydrolysis of esters, has shown a second-order rate constant of 0.13 ± 0.01 M^{-1} s^{-1} in 10% (v/v) CH_3CN at 25 °C in 4-nitrophenyl acetate (NA) hydrolysis, which is almost the same as the corresponding value for the very reactive alcohol-pendent [12]aneN_3−Zn complex. Present work shows for the first time that Zn(II) complexes of the asymmetric tripodal polyamine bearing an ethoxyl pod can also serve as good models of Zn(II)-containing enzymes.

Introduction

The role of Zn(II) in the activation of the coordinated alcoholic OH or water molecule and that of the following Zn(II)-bound alkoxide or hydroxide in the hydrolytic process have been hot spots in the field of bioinorganic chemistry recently.[1−5] Zn(II)-bound alkoxides or hydroxides, derived from the deprotonation of the Zn(II)-bound external water or internal alcoholic residues (e.g., serine, theronine) in Zn(II)-containing enzymes, usually act as nucleophiles to attack electrophilic substrates (CO_2, carboxy esters, phosphates, and peptide amides). For example, in carbonic anhydrase (CA) the Zn(II)-bound water deprotonates in physiological pH to yield nucleophilic hydroxide to attack the carbon atom in CO_2.[6,7] Another example is alkaline phosphatase, in which the Zn(II)-activated serine(102) deprotonates and serves as an initial nucleophile to attack the phosphate to yield a phosphoseryl−enzyme intermediate, which is then attacked again by the adjacent Zn(II)-bound hydroxide to recycle the hydrolysis.[8,9]

In the past 20 years, systematical modeling studies on the intrinsic chemical properties of Zn(II) ions in biological system have been conducted by Kimura[10−17] and other chemists.[18−34] In these significant works, many intriguing and convincing pictures about the essential role of Zn(II)−serine alkoxide in Zn(II)-involving serine enzymes have been provided, along with which a series of novel Zn(II)−polyamine complexes with fast hydrolysis rate have been reported. However, most of these

* Corresponding author. Telephone: +86-25-3595706. Fax: +86-25-3314502. E-mail: wxtang@netra.nju.edu.cn.
[†] Nanjing University.
[‡] Chengdu Branch of the Chinese Academy of Sciences.

(1) Vallee, B. L.; Auld, D. S. *Acc. Chem. Res.* **1993**, *26*, 543.
(2) Suh, J. *Acc. Chem. Res.* **1992**, *25*, 273.
(3) Lipscome, W. N.; Strater, N. *Chem. Rev.* **1996**, *96*, 2396.
(4) Bertini, I.; Luchinat, C.; Rosi, M.; Sgamellotti, A.; Tarantelli, F. *Inorg. Chem.* **1990**, *29*, 1460.
(5) Canary, J. W.; Xu, J.; Castagnetto, J. M.; Rentzeperis, D.; Marky, L. A. *J. Am. Chem. Soc.* **1995**, *117*, 11545.
(6) Silverman, D. N.; Lindskog, S. *Acc. Chem. Res.* **1988**, *21*, 30.
(7) Nair, S. K.; Christianson, D. W. *J. Am. Chem. Soc.* **1991**, *113*, 9455.
(8) Kim. E. E.; Wyckoff, H. W. *J. Mol. Biol.* **1991**, *218*, 449.
(9) Coleman, J. E. *Annu. Rev. Biophys. Biomol. Struct.* **1992**, *21*, 441.
(10) Koike, T.; Takamura, M.; Kimura, E. *J. Am. Chem. Soc.* **1994**, *116*, 8443.
(11) Koike, T.; Kajitani, S.; Nakamura, I.;. Kimura, E.; Shiro, M. *J. Am. Chem. Soc.* **1995**, *117*, 1210.
(12) Kimura, E.; Nakamura, I.; Koike, T.; Shionoya, M.; Kodama, Y.; Ikeda, T.; Shiro, M. *J. Am. Chem. Soc.* **1994**, *116*, 4764.
(13) Kimura, E.; Shionoya, M.; Hoshino, A.; Ikeda, T.; Yamada, Y. *J. Am. Chem. Soc.* **1992**, *114*, 10134.
(14) Koike, T.; Kimura, E. *J. Am. Chem. Soc.* **1991**, *113*, 8935.
(15) Kimura, E.; Shiota, T.; Koike, T.; Shiro, M.; Kodama, M. *J. Am. Chem. Soc.* **1990**, *112*, 5805.
(16) Kimura, E.; Yamaoka, M.; Morioka, M.; Koike, T. *Inorg. Chem.* **1986**, *25*, 3883.
(17) Kimura, E.; Koike, T.; Toriumi, K. *Inorg. Chem.* **1988**, *27*, 3687.
(18) Sigman, D. S.; Jorgensen, C. T. *J. Am. Chem. Soc.* **1972**, *94*, 1724.
(19) Gellman, S. H.; Petter, R.; Breslow, R. *J. Am. Chem. Soc.* **1986**, *108*, 2388.
(20) Weijnen, J. G.; Koudijs, A. *J. Org. Chem.* **1992**, *57*, 7258.
(21) Looney, A.; Han, R.; McNeill, K.; Parkin, G. *J. Am. Chem. Soc.* **1993**, *115*, 4690.
(22) Xu, X.; Lajmi, A. R.; Canary, J. W. *J. Chem. Soc., Chem. Commun.* **1998**, 2701.
(23) Greener, B.; Moore, M. H.; Walton, P. H. *J. Chem. Soc., Chem. Commun.* **1996**, 27.
(24) Breslow, R.; Berger, D.; Huang, D.-L. *J. Am. Chem. Soc.* **1990**, *112*, 3686.
(25) Hay, R. W.; Govan, N. *J. Chem. Soc., Chem. Commun.* **1990**, 714.
(26) Ruf, M.; Weis, K.; Vahrenkamp. H. *J. Chem. Soc., Chem. Commun.* **1994**, 135.
(27) Suh, J.; Park, T. J.; Hwang, B. K. *J. Am. Chem. Soc.* **1992**, *114*, 5141.
(28) De Rosch, M. A.; Trogler. M. C. *Inorg. Chem.* **1990**, *29*, 2409.
(29) Hikichi, S.; Tanaka, M.; Moro-oka, Y.; Kitajima, N. *J. Chem. Soc., Chem. Commun.* **1992**, 814.
(30) Murthy, N. N.; Karlin, K. D. *J. Chem. Soc., Chem. Commun.* **1993**, 1236.
(31) Chapman, W. H, Jr.; Breslow, R. *J. Am. Chem. Soc.* **1995**, *117*, 5462.
(32) Koike, T.; Inoue, M.; Kimura, E.; Shiro, M. *J. Am. Chem. Soc.* **1996**, *118*, 3091.
(33) Clewley, R. G.; Slebocka-Tilk, H.; Brown, R. S. *Inorg. Chim. Acta* **1989**, *157*, 233.
(34) Tsubouchi. A.; Bruice, T. C. *J. Am. Chem. Soc.* **1994**, *116*, 11614.

10.1021/ic000642n CCC: $20.00
Published on Web 04/13/2001

Chart 1

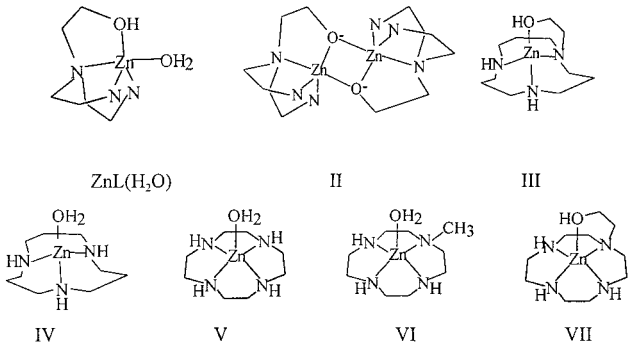

ligands used were confined to macrocyclic polyamines and those with a ethoxyl pendent[10−17] (as illustrated in Chart 1, **III**−**VII**) and few of the former research works have been concentrated on tripodal polyamines bearing an ethoxyl pod. We hold the opinion that the tripods should have some advantages over the macrocyclic polyamines. As shown in Chart 1, the tripodal ligands often construct a trigonal-dipyramidal environment around the captured metal ion, leaving the fifth coordination point vacant, which facilitates the ligation of free solvent molecular or the substrates in catalytic process, while, comparatively, the macrocyclic ligands tends to be more rigid in coordination modes.

To elucidate whether the tripodal polyamine with an ethoxyl pod can mimic the chemical surroundings of Zn(II) in the active site of the Zn(II)-containing enzymes and also to seek better and more practical hydrolysis catalysts, herein we studied and reported the protonation constants of a tripodal polyamine bearing an alcoholic pod, 2-[bis(2-aminoethyl)amino]ethanol, for the first time and investigated its complexation behavior with Zn(II) in the solution. It is found that when ligated to Zn(II) ion, the alcoholic OH deprotonates with a very low pK_a of 7.7 to give an alkoxide Zn(II)−$^-$OR complex. The monomeric complex **I** with the alcoholic group partially deprotonated and the dimeric alkoxide-coordinating complex **II** as the first M−L complexes were proven by X-ray diffraction. Furthermore, study on the hydrolysis of a carboxy ester, 4-nitrophenyl acetate (NA), promoted by the ZnL complex suggested that the Zn(II)-bound alkoxide ranks among those strongest nucleophiles ever found. Present work shows for the first time that the asymmetric tripodal heteropolyamines bearing an ethoxyl pod and its Zn(II) complexes can also be good models of Zn(II)-containing enzymes.

Experimental Section

Materials. 2-[Bis(2-aminoethyl)amino]ethanol, the title ligand L, was synthesized as described previously in the literature.[35] The other reagents were of analytical grade from commercial sources and were used without any further purification.

$[ZnH_{-0.25}L(H_2O)](ClO_4)_{1.75}$ (I). To a solution containing 0.85 g (5.8 mmol) of L and 3 mL of CH_3CN was added 2.16 g (5.8 mmol) of $Zn(ClO_4)_2\cdot 6H_2O$ bit by bit, while being cooled by an ice−water mixture. After being stirred for 10 min, the solution was filtered and the filtrate was placed in the air to evaporate. A few days later, colorless prisms were obtained in 37% yield. Anal. Calcd for $C_6H_{18.75}N_3O_9Cl_{1.75}Zn$: C, 17.8; H, 4.7; N, 10.4; Zn, 16.2. Found: C,17.6; H, 4.5; N, 10.5; Zn, 16.2.

$[Zn_2(H_{-1}L)_2](ClO_4)_2$ (II). A 0.16 g (1.1 mmol) amount of L was dissolved in 1 mL of water, to which 0.14 g (1.1 mmol) of $ZnCl_2$ was added with stirring. Then, 1 mL of saturated $NaClO_4$ solution was added to the solution, from which a white residue was obtained. The residue was filtered out and dissolved in 5 mL of CH_3CN. Colorless prisms crystallized when the CH_3CN solution was diffused by ether. Anal. Calcd for $C_{12}H_{32}O_{10}Cl_2Zn_2$: C, 23.2; H, 5.2; N, 13.5. Found: C, 23.5; H, 5.2; N, 13.2.

Caution! Perchlorate salts of compounds containing organic ligands are potentially explosive especially when heated or bumped. Only small quantities of these compounds should be prepared and handled behind suitable protective shields.

Potentiometry. Potentiometric studies were conducted with an Orion 91-04 glass combination pH electrode and an Orion microprocessor ionalyzer/901 at 25 °C. All solutions were carefully protected from air by a stream of humidified nitrogen gas. Standard NaOH (CO_2 free) was added by a spiral micro-injector. $Zn(SO_4)_2$ solution was calibrated by standard EDTA. And double-distilled water with a pH value about 6 is used. Temperature of the cell was controlled by a thermostat. The system was calibrated with dilute standard acid and alkali solution. K_w was chose as 13.69 for 25 °C. A 0.1 M NaCl solution was used to adjust the ionic strength to 0.1. Solutions containing 1 mmol L with or without equimolar $Zn(SO_4)_2$ were titrated to pH > 11. The complexation and protonation constants were calculated using the program BEST.[38] All data represent the average of at least two independent experiments, and all the σ fit values have been reduced to less than 0.019 after optimization.

Kinetic Studies. 4-Nitrophenyl acetate (NA) hydrolysis was carried out by a UV−vis spectral method using a Shimadzu UV-240 spectrophotometer with a thermostat to control the temperature (±0.5 °C). The NA solution was added by micro-injector of 100 μL volume. The hydrolysis of NA (1.0−2.0 mM) was followed at $I = 0.10$ (90 mM $NaNO_3$) and pH 8.09, 8.55, and 8.90 (20 mM Tris·HCl buffers) in 10% (v/v) CH_3CN aqueous solution, by the release of 4-nitrophenolate (NP) at 400 nm. An initial slope method has been applied on the data processing procedure. Experiments were conducted at least in duplicate.

X-ray Crystallographic Study of I and II. Intensities data for the crystals of **I** and **II** were collected on a Siemens P4 four-circle diffractometer with monochromated Mo Kα ($\lambda = 0.710\ 73$ Å) radiation using the $\omega/2\theta$ scan mode at 20 °C in the rang $1.77° \le \theta \le 24.97°$ for **I** and at 23 °C in the rang $1.99° \le \theta \le 26.50°$ for **II**, respectively. An empirical absorption correction based on ψ scans was applied. Data were corrected with Lorentz and polarization effects during data reduction using XSCANS.[36] The structure was solved by direct methods and refined using SHELXL97 software.[37] All non-hydrogen atoms were refined anisotropically by full-matrix least squares.

For crystals of **I**, N2 and O6 are disordered, with occupancy factors of 0.66 and 0.33, respectively, and were refined with the same coordinates and anisotropic thermal parameters. In the O6 position, ROH:RO$^-$ should be 3:1 since the ratio of ClO_4^-:Zn for Cl(2) is found to be 1:1, while ClO_4^-:Zn ratio for another perchlorate anion Cl(1) unit is 0.75:1. The H atoms for disordered OH and NH_2 were not located. We also attempted to solve the structure supposing the coordinated water instead of the alcoholic hydroxyl group deprotonates. However, we abandoned this possibility finally, because it seems to be unreasonable in both chemistry and crystallography, as described below. The coordinated water molecules O1w, $O1w^I$, and $O1w^{II}$ are also disordered around the 3-fold axis with occupancy factors of 0.33. One perchlorate anion for Cl(2) unit is disorder with occupancy factors for O1, O2, and O3 being 0.33, so the thermal parameters of O atoms and the Cl−O bond lengths were restrainted.

Hydrogen atoms for the carbon atoms of both **I** and **II** were placed in their calculated position with C−H = 0.96 Å, assigned fixed isotropic thermal parameters (1.2 times that of the atom they attached), and

(35) Bobylev, V. A.; Chechik, V. D. *Zh. Obshch. Khim.* **1990**, *60*, 2721.

(36) *XSCANS (Version 2.1)*; Siemens Analytical X-ray Instruments Inc.: Madison, WI, 1994.

(37) Sheldrick, G. M. *SHELXTL 97, Program for Crystal Structure Determinations*; University of Göttingen: Göttingen, Germany, 1997.

(38) Martell, A. E.; Motekaitis, R. J. *Determination and Use of Stability Constants*, 2nd ed.; VCH Publishers: New York, 1992.

Table 1. Crystallographic Data for Monomeric **I** and Dimeric **II**

	I	**II**
formula	$C_6H_{18.75}Cl_{1.75}N_3O_9Zn$	$C_{12}H_{32}Cl_2N_6O_{10}Zn_2$
fw	404.40	622.08
cryst system	cubic	orthorhombic
space group	$P\bar{4}3m$	Pbca
T/K	293(2)	296(2)
λ/Å	0.710 73	0.710 73
color of cryst, habit	colorless, prism	colorless, prism
a/Å	11.5126(9)	14.657(2)
b/Å	11.5126(9)	11.234(2)
c/Å	11.5126(9)	28.677(5)
$\alpha = \beta = \gamma$/deg	90	90
V/Å^3	1525.9(2)	4721.9(13)
Z	4	8
ρ_{calcd}/g cm^{-3}	1.760	1.750
μ/mm^{-1}	1.960	2.317
cryst size/mm	0.28 × 0.28 × 0.28	0.48 × 0.44 × 0.44
θ range/deg	1.77−24.97	1.99−26.50
reflns collcd	396	4892
independt reflns	351 (R_{int} = 0.0659)	3275 (R_{int} = 0.0380)
max and min transm	0.2834 and 0.2404	0.4651 and 0.4301
data/restraints/params	396/45/64	4892/0/290
GOF on F^2	1.128	0.907
R1[a] [$I > 2\sigma(I)$]	0. 0659	0.0380
WR2 [$I > 2\sigma(I)$]	0.1853[b]	0.0916[c]

[a] $R1 = \Sigma||F_o| - |F_c||/\Sigma|F_o|$; $wR2 = |\Sigma w(|F_o|^2 - |F_c|^2)|/\Sigma|w(F_o)^2|^{1/2}$. [b] $w = 1/[(F_o^2)^2 + (0.1219P)^2 + 2.0089P]$, where $P = (F_o^2 + 2F_c^2)/3$. [c] $w = 1/[(F_o^2)^2 + (0.0557P)^2 + 0.0000P]$, where $P = (F_o^2 + 2F_c^2)/3$.

allowed to ride on their respective parent atoms. Hydrogen atoms of the water molecules in **I** were found from the difference Fourier maps and also assigned fixed isotropic thermal parameters. Hydrogen atoms for N2 and O6 were not located because of disorder. The relevant crystal data and structural parameters for complexes are summarized in Table 1.

Physical Measurements. Elemental analysis was performed on a Perkin-Elmer 240C. ES-MS spectra were obtained from a Finnigan MAT LCQ ES mass spectrometer with a mass to charge (m/z) range of 2000. A mixture of 1:1 CH_3OH and water was used as the solvent, and the concentration used in the experiment was 1.0 μmol L^{-1}. ^{1}H NMR spectra were recorded on the Bruker AM 500 spectrometer.

Results and Discussion

Protonation and Zn(II) Complexation Constants of L. The protonation and Zn(II) complexation constants of the polyamine L are determined by potentiometric titration for the first time. A typical titration curve of 1.0 mM L with 3 equimolar HCl by 0.1 M NaOH solution at 25 °C is shown in Figure 1a. The titration data are analyzed for equilibria 1−3. The protonation constants K_1−K_3 are defined as follows:

$$L + H^+ \rightleftharpoons HL \quad K_1 = [HL]/[L]a_{H^+} \tag{1}$$

$$HL + H^+ \rightleftharpoons H_2L \quad K_2 = [H_2L]/[HL]a_{H^+} \tag{2}$$

$$H_2L + H^+ \rightleftharpoons H_3L \quad K_3 = [H_3L]/[H_2L]a_{H^+} \tag{3}$$

The obtained association constants are listed in Table 2.

When equimolar Zn(II) was added to the solution, the titration curve reveals a very long pH buffering range between pH 5.5 and 9 (a = 1.0−4.5), as shown in Figure 1b, which implies the formation of ZnL and $ZnH_{-1}L$. Four species, ZnL, $ZnH_{-1}L$, $ZnH_{-1}L(OH)$, and $Zn_2(H_{-1}L)_2$, were believed to exist in aqueous solution, owing to the following crystal X-ray analysis and ES-MS experiments.

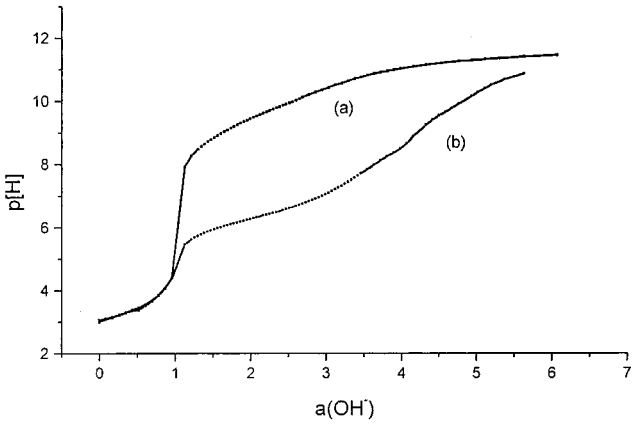

Figure 1. Typical titration curve for L·3HCl at 25 °C and I = 0.1 (NaCl): (a) 1.0 mM L·3HCl, σ fit 0.017 after optimization by BEST; (b) 1.0 mM L·3HCl + 1.0 mM $ZnSO_4$, σ fit 0.018 after optimization by BEST.

Table 2. Comparison of Protonation Constants of L and Other Macrocyclic and Tripodal Ligands and Their Complexation Constants with Zn(II)[a]

	L	alcohol-pendent [12]aneN$_3$[b]	tren[c]	phenol-pendent [12]ane N$_3$[d]
log K_1	10.00(0.03)	11.7	10.43	9.67
log K_2	9.02(0.03)	6.92	9.87	7.09
log K_3	3.36(0.05)	2.2	9.01	2.0
log K(ZnL)	9.41(0.06)	7.6	15.20	8.8
pK_{a1}	7.74(0.02)	7.4	10.68	6.8
pK_{a2}	9.78(0.25)			10.7
log K_d	0.9(0.3)	0.8(0.3)		

[a] $K_n = [H_nL]/([H_{n-1}L]a_{H^+})$, K(ZnL) = [ZnL]/([L][Zn(II)]), K_{a1} = $[ZnH_{-1}L]a_{H^+}/[ZnL]$, K_{a2} = $[ZnH_{-1}L(OH)]a_{H^+}/[ZnL]$, and K_d = $[(ZnL_{-H})_2]/[ZnL_{-H}]^2$, at I = 0.1 (NaCl) and 25 °C. [b] From ref 12 at I = 0.1 ($NaNO_3$) and 25 °C. [c] From ref 5 at I = 1 ($NaClO_4$) and 25 °C. [d] There is one additional deprotonation constant of ∼13, defined by K = $[L]/[H_{-1}L]a_{H^+}$ due to the high acidity of the phenol group of the ligand. From refs 16 and 17 at I = 0.1 ($NaClO_4$), and 25 °C.

The complexation constants of L with Zn(II), i.e., K(ZnL), K_a, and K_d, are defined as follows:

$$L + Zn^{2+} \rightleftharpoons ZnL \quad K(ZnL) = [ZnL]/[L][Zn^{2+}] \tag{4}$$

$$ZnL \rightleftharpoons ZnH_{-1}L + H^+ \quad K_{a1} = [ZnH_{-1}L]a_{H^+}/[ZnL] \tag{5}$$

$$ZnH_{-1}L \rightleftharpoons ZnH_{-1}L(OH) + H^+ \quad K_{a2} = [ZnH_{-1}L(OH)]a_{H^+}/[ZnH_{-1}L] \tag{6}$$

$$2ZnH_{-1}L \rightleftharpoons Zn_2(H_{-1}L)_2 \quad K_d = [Zn_2(H_{-1}L)_2]/[ZnH_{-1}L]^2 \tag{7}$$

To rationalize the model selection and data process, several different analysis processes were conducted and evaluated: In the first case, the deprotonation species was set to be the monomer only; i.e., eqs 4−6 were included. In the second case, the dimer only was used, which contained ZnL and $Zn_2(H_{-1}L)_2$, with/without the double-deprotonated species $ZnH_{-1}L(OH)$. In the third case, both the dimer and monomer were contained, i.e., eqs 4−7. In the first and third cases, reasonable results were given by BEST, with σ fit values optimized to be 0.018 and the β values almost the same, respectively; however, in the second case where only the dimer was employed, great deviation occurred (σ fit 0.037 and 0.055, and all the deviations of the calculated and recorded pH values were large, especially in the high-pH region). Since the occupancy factor of the dimer is

Chart 2

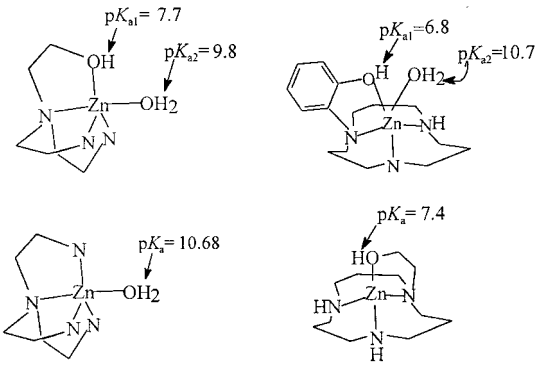

Scheme 1

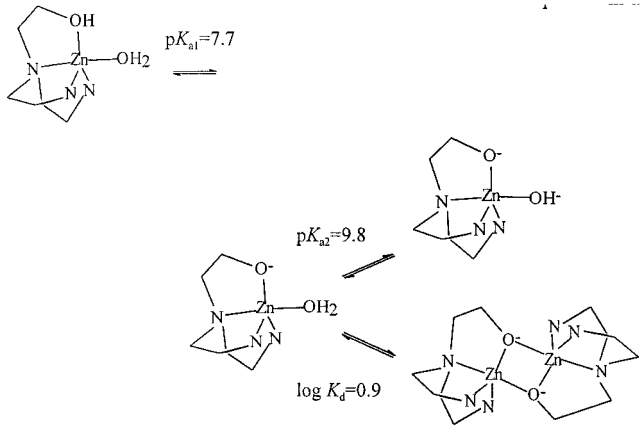

less than 2%, the consistency of the first and third data process is reasonable. Accordingly, we chose the third case as the most rational one.

The constants for log *K*(ZnL) and the deprotonation constants, pK_a's at 25 °C together with the values measured previously for related systems, are also included in Table 2. The deprotonation of the alcoholic OH group (pK_{a1} = 7.7) for the present ligand is promoted by its binding to Zn(II), which then renders the basicity of Zn(II)−OH_2 higher (pK_{a2} = 9.8), as established by the pH-metric titration. The present results are comparative with another well-established example of stepwise deprotonation in [Zn(phenol-pendent [12]aneN_3)(H_2O)].[16,17] Also, the deprotonation constant of the Zn(II)-bound alcoholic group (pK_{a1} = 7.7) is almost the same as but a little bit higher than that in **III**, 7.4;[12] the pK_a value of Zn(II)-bound water, 9.8, is similar with that found in Zn(tren)(H_2O), 10.68,[5,39] as illustrated in Chart 2 and Table 2. The 1:1 ZnL complex, its deprotonation mode, and association mode present in aqueous solution can be depicted as in Scheme 1 for clarity.

Electrospray mass spectroscopy (ES-MS) data obtained for complex **I** indicate the formation of 1:1 complexes $[ZnH_{-1}L]^+$, $[ZnL(CH_3COO)]^+$, and $[ZnL(ClO_4)]^+$ in aqueous solution, and no peaks corresponding to $[ZnL(OH^-)]^+$ and $[Zn_2(H_{-1}L)_2]^{2+}$ are found in the spectra. Comparisons of the calculated and observed electrospray MS of selected peaks in the cation region are presented in Figure 3. According to this, $ZnH_{-1}L$ is believed to be the major deprotonated species present in the solution instead of $ZnL(OH^-)$ at near neutral pH. The conclusive structure for the dimer **II**, which was isolated from a more concentrated solution of $Zn(ClO_4)_2$ and ligand, comes from elemental analysis and the following X-ray crystal analysis.

(39) Anderegg, G.; Gramlich, V. *Helv. Chim. Acta* **1994**, *77*, 685.

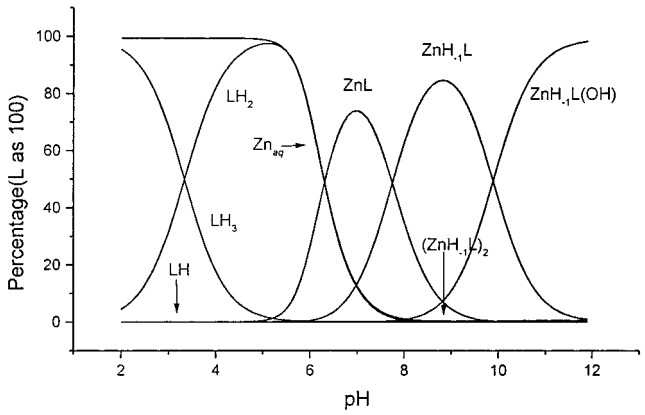

Figure 2. Species distribution graph as a function of pH for the 1 mM L + 1 mM Zn(II) system at 25 °C and I = 0.1 (NaCl). $(ZnH_{-1}L)_2$ stands for the dimer **II**.

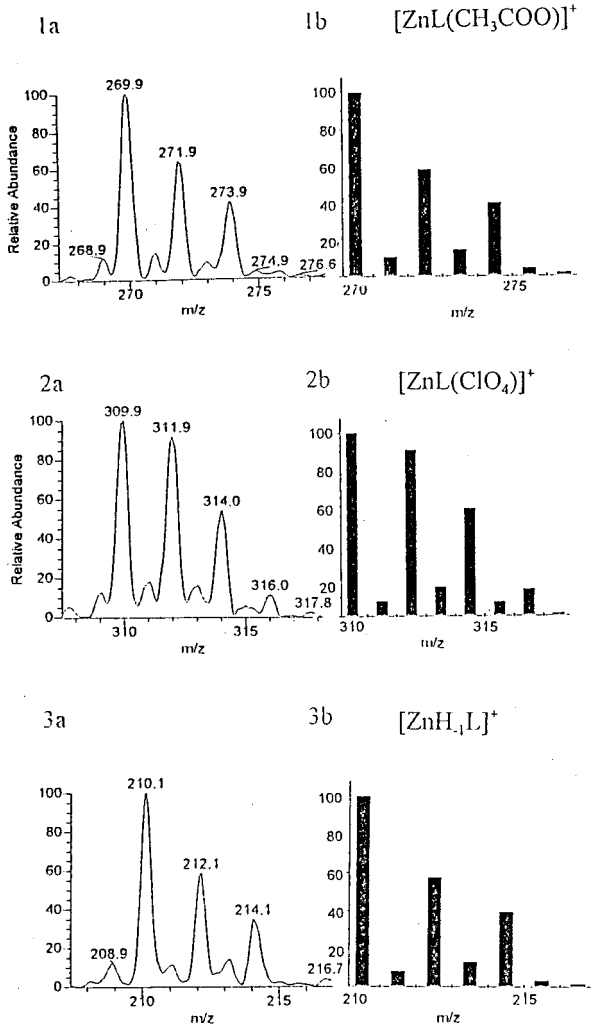

Figure 3. ES-MS spectra of (1a) observed and (1b) calculated patterns for $[ZnL(CH_3COO)]^+$, (2a) observed and (2b) calculated patterns for $[ZnL(ClO_4)]^+$, and (3a) observed and (3b) calculated patterns for $[ZnH_{-1}L]^+$.

A typical diagram for species distribution as a function of pH at [total Zn(II)] = [total L] = 1 mM and 25 °C is displayed in Figure 2. It is found that although the stability of ZnL complex with a complexation constant of 9.41 is inferior to that of **III**, **VI**, and **VII**, ZnL remains as the major Zn(II)-containing species with the maximum occupancy of 73.9% at pH = 7.0.

Table 3. Selected Bond Distances and Angles for **I**[a]

Zn1−N2	2.015(7)	Zn1−O6^{I}	2.015(7)
Zn1−O6^{II}	2.015(7)	Zn1−N2^{I}	2.015(7)
Zn1−N2^{II}	2.015(7)	Zn1−O1w	2.158(16)
Zn1−O1w^{I}	2.158(16)	Zn1−O1w^{II}	2.158(16)
Zn1−N1	2.180(8)		
O6^{I}−Zn1−N2	118.43(9)	O6^{II}−Zn1−N2	118.43(9)
O6^{I}−Zn1−O6^{II}	118.43(9)	N2−Zn1−N2^{I}	118.43(9)
N2^{I}−Zn1−O6^{I}	0.0(4)	O6^{II}−Zn1−N2^{I}	118.43(9)
N2−Zn1−N2^{II}	118.43(9)	O6^{I}−Zn1−N2^{II}	118.43(9)
O6^{II}−Zn1−N2^{II}	0.0(4)	N2^{I}−Zn1−N2^{II}	118.43(9)
N2−Zn1−O1w	73.2(5)	O6^{I}−Zn1−O1w	108.5(3)
O6^{II}−Zn1−O1w	108.5(3)	N2^{I}−Zn1−O1w	108.5(3)
N2^{II}−Zn1−O1w	108.5(3)	N2−Zn1−O1w^{I}	108.5(3)
O6^{I}−Zn1−O1w^{I}	73.2(5)	O6^{II}−Zn1−O1w^{I}	108.5(3)
N2^{I} −Zn1−O1w^{I}	73.2(5)	N2^{II}−Zn1−O1w^{I}	108.5(3)
N2−Zn1−O1w^{II}	108.5(3)	O6^{I}−Zn1−O1w^{II}	108.5(3)
O6^{II}−Zn1−O1w^{II}	73.2(5)	N2^{I-}Zn1−O1w^{II}	108.5(3)
N2^{II}-Zn1O1w^{II}	73.2(5)	N2 Zn1N1	82.8(2)
O6^{I}−Zn1−N1	82.8(2)	O6^{II}−Zn1−N1	82.8(2)
N2^{I} -Zn1N1	82.8(2)	N2^{II}-Zn1N1	82.8(2)
O1w−Zn1−N1	156.0(4)	O1w^{I}−Zn1−N1	156.0(4)
O1w^{II}−Zn1−N1	156.0(4)		

[a] Symmetry transformations used to generate equivalent atoms: I, *y*, *z*, *x*; II, *z*, *x*, *y*.

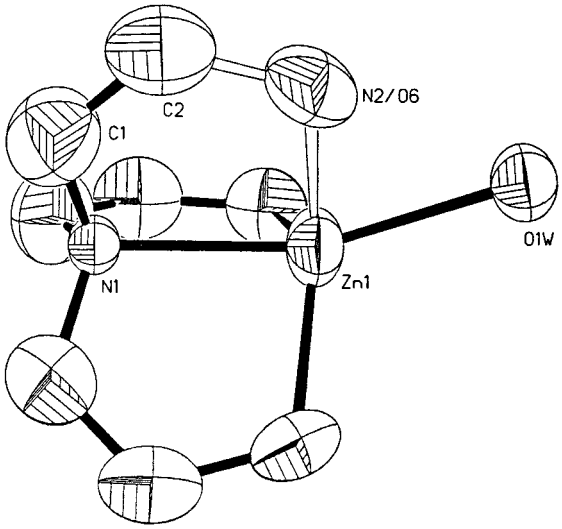

Figure 4. ORTEP drawing (30% probability ellipsoids) of the monomer **I**. All hydrogen atoms bonded to carbon and perchlorate anions are omitted for clarity.

At weak alkaline range, $ZnH_{-1}L$ soon reaches the highest occupancy of 84.7% at pH 8.8. When pH value is more than 10.8, the double-deprotonated species $ZnH_{-1}L(OH)$ becomes the major Zn(II)-containing species.

X-ray Structure of the Monomeric Complex $[ZnH_{-0.25}L(H_2O)](ClO_4)_{1.75}$ (I). The monomeric complex was crystallized from CH_3CN. The elemental analysis and ICP zinc analysis suggested the formula between the protonated and deprotonated species, similar to $C_6H_{18.75}N_3O_9Cl_{1.75}Zn$, which seems to be puzzling. The X-ray crystal analysis finally gives a satisfying explanation by postulating the disorder of alcoholic OH and O with a ratio of 3:1. Selected bond distances and angles are given in Table 3.

Zn and N1 atoms are located on the 3-fold axis. A distorted trigonal-bipyramidal environment formed by the four coordinating atoms (N_3O of the tripod) and an external water molecular around Zn(II) has been illustrated in Figure 4. The Zn(II) atom lies 0.2541 Å above the trigonal equatorial plane formed by the terminal N and O atoms of the tripod with equal N2/O6−Zn1−N2^{I}, N2/O6−Zn1−N2^{II}, and N2^{I}-Zn1−N2^{II} angles being 118.43°, while the two axial sites are occupied by apical N atom of the tripod and an external water with a N1−Zn−O1w angle of 156°. The distortion (Δ) of the coordination polyhedron from a regular trigonal-bipyramid ($\Delta = 0$) to the tetragonal pyramid ($\Delta = 1$) has been calculated according to the literature reported by Mutterties and Galy.[40,41] The value of 0.11 indicates that the geometry of coordination around the Zn(II) are much closer to TBP. The Zn−N and Zn−O(alcohol) bonds, 2.015 Å, are shorter than the average distance of 2.124 Å in dimeric alcohol-pendent [12]aneN_3 Zn(II) complex[12] and 2.125 Å in dimeric $[Zn_2(H_{-1}L)_2](ClO_4)_2$ (**II**) illustrated below. The axial Zn1−N1 and Zn1−O1w bonds are elongated to 2.180 and 2.158 Å comparing with the equatorial Zn−N and Zn−O bonds.

Table 4. Selected Bond Distances and Angles for **II**

Zn1···Zn2	2.9652(6)	Zn1−O2	1.982(2)
Zn1−O1	2.021(2)	Zn1−N1	2.244(3)
Zn1−N2	2.042(3)	Zn1−N3	2.088(3)
Zn2−O1	2.005(2)	Zn2−O2	2.018(2)
Zn2−N4	2.255(3)	Zn2−N5	2.077(3)
Zn2−N6	2.044(3)		
O2−Zn1−O1	83.69(10)	O2−Zn1−N2	110.62(12)
O1−Zn1−N2	115.52(12)	O2−Zn1−N3	101.22(12)
O1−Zn1−N3	124.77(12)	N2−Zn1−N3	113.68(14)
O2−Zn1−N1	162.90(12)	O1−Zn1−N1	81.10(11)
N2−Zn1−N1	83.16(13)	N3−Zn1−N1	81.32(13)
O2−Zn1−Zn2	42.62(7)	O1−Zn1−Zn2	42.36(7)
N2−Zn1−Zn2	129.89(9)	N3−Zn1−Zn2	113.15(10)
N1−Zn1−Zn2	120.73(9)	O1−Zn2−O2	83.19(10)
O1−Zn2−N6	110.28(13)	O2−Zn2−N6	110.69(13)
O1−Zn2−N5	101.84(12)	O2−Zn2−N5	123.05(12)
N6−Zn2−N5	119.61(15)	O1−Zn2−N4	161.64(11)
O2−Zn2−N4	80.16(11)	N6−Zn2−N4	83.02(13)
N5−Zn2−N4	81.09(13)	O1−Zn2−Zn1	42.78(7)
O2−Zn2−Zn1	41.70(7)	N6−Zn2−Zn1	126.03(12)
N5−Zn2−Zn1	112.48(10)	N4−Zn2−Zn1	119.22(9)

X-ray Structure of the Dimer $[Zn_2(H_{-1}L)_2](ClO_4)_2$ (II). As shown in distribution diagram given by pH potentiometric titration, the dimeric species has the maximum occupancy of only 1.9% in pH 8.5 of all the Zn(II)-containing species. Fortunately enough, we crystallized it and got the dimeric structure by X-ray diffraction. Selected bond distances and bond angles are listed in Table 4.

Both Zn(II) atoms in the dimer are pentacoordinated with the coordination surroundings of a distorted trigonal-bipyramid by the three N atoms and one internal O, one intermolar O atom from another ligand serving as bridging group. Zn1 and Zn2 atoms are located 0.2846 and 0.2981 Å above the two equatorial planes formed by O1, N2, N3 and O2, N5, N6, respectively. The axial coordination atoms are approximately linear with the central Zn atoms with O2−Zn1−N1 = 162.90° and O1−Zn2−N4 = 161.64°, respectively. The two equatorial planes are somewhat parallel with a dihedral angle of 22.0°. Additionally, the two Zn(II) atoms and two bridging O^{-} anions, namely Zn1, Zn2, O1, and O2, are approximately in a plane with a maximum deviation of 0.106 Å from the mean plane.

Though coordination surroundings around both Zn(II) atoms are similar, a significant difference occurs: the Zn2 subunit has Δ of 0.11 and in the Zn1 subunit $\Delta = 0.27$, indicating that the geometry of the Zn2 coordination polyhedron is closer to TBP.[40,41]

(40) Muetterties, E. L.; Guggenberger, L. J. *J. Am. Chem. Soc.* **1974**, *96*, 1748.
(41) Galy, J.; Bonnet, J. J.; Andersson, S. *Acta Chem. Scand.* **1979**, *33*, 383.

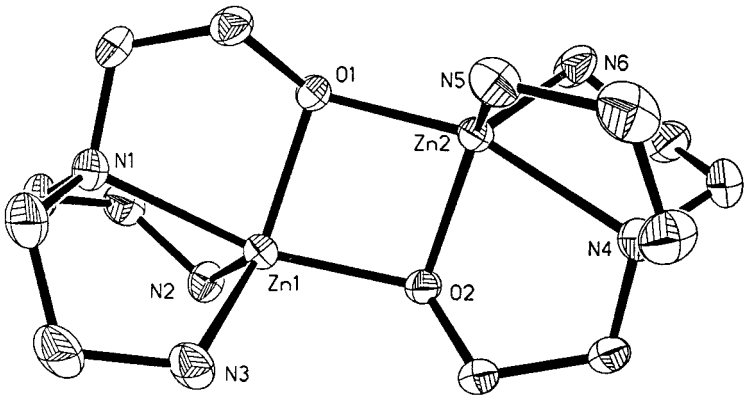

Figure 5. ORTEP drawing (30% probability ellipsoids) of the dimer **II**. All hydrogen atoms bonded to carbon and perchlorate anions are omitted for clarity.

Comparison of the structure with the former dimer, dimeric alcohol-pendent [12]aneN_3–Zn complex, shows that the bond distances are matching: the averaged Zn−N distances are 2.124 and 2.125 Å, respectively, with elongated Zn−apical N atom of 2.250 Å vs 2.259 Å.[12] However, X-ray diffraction analysis reveals a very short Zn−Zn distance of 2.965 Å in **II**, almost the shortest among all those dinuclear Zn(II) complexes, comparing with that in [((2-pyridyl)$_3$N)Zn(μ-OH)$_2$Zn((2-pyridyl)$_3$N)], 2.99 Å,[30] in dimeric alcohol-pendent [12]aneN_3, 3.16 Å,[12] and in the dinuclear complex Zn_2(26-oxy-1,4,7,10,13,16,19,22-octaazabicyclo[11.11.3]heptacodane), 3.42 Å.[32] It is believed that in the present structure there is significant metal−metal interaction taking effect. Also the intermolar Zn−O distance is shorter than the intramolar Zn−O distance (for Zn1, 1.982 Å vs 2.021 Å;for Zn2, 2.005 Å vs 2.018 Å), but in alcohol-pendent [12]aneN_3–Zn(II) dimer, the structure shows the reverse (2.079 Å vs 1.95 Å).[12] This founding leads to the conclusion that since the intermolar and intramolar oxygen are shared by the two Zn(II) ions, it is not necessary that the external RO−-Zn(II) interaction should be weaker.

4-Nitrophenyl Acetate (NA) Hydrolysis Promoted by ZnL. As a model for the active center in Zn(II)-containing hydrolytic enzymes, especially alkaline phosphatase, the catalytic activity of the ZnL complex has been tested. Since the phosphomonoesters underwent extremely slow hydrolysis with ZnL as with other N_3O−Zn(II) complexes (**III**−**VII**), the carboxy ester 4-nitrophenyl acetate (NA) was used as substitute.[12,15,42] We followed the hydrolysis of NA (1.0−2.0 mM) promoted by ZnL (**I**, calculated as monomeric species) with concentrations varying from 0.4 to 1.6 mM at $I = 0.10$ (90 mM $NaNO_3$) and pH 8.09, 8.55, and 8.90 (20 mM Tris·HCl buffers) in 10% (v/v) CH_3CN aqueous solution at 25 °C, by the release of 4-nitrophenolate (NP) at 400 nm. An initial slope method has been applied on the data processing procedure, as previously described in the literature. The initial rate constant k_{in}, observed rate constant k_{obs}, and second-order rate constant k_{NA} are defined as follows:[42]

$$v_{Zn} = k_{in}[NA]$$
$$= (k_{obs}[\text{total Zn(II) complex}] + k_{OH}[OH^-] + ...)[NA]$$
$$= (k_{NA}[ZnH_{-1}L] + k_{OH}[OH^-] + ...)[NA]$$

By following the absorbance increases up to 5% of the reactions, one can measure the initial velocities (v_{Zn}). Since the substrate concentrations ([NA] = 1.0−2.0 mM) were essentially kept constant during the measurement, the absorbance increases linearly (correlation coefficient >0.99) with the slope being v_{Zn}. Initial rate constant k_{in} was calculated from the slope of the straight line v_{Zn} vs [NA]. This indicates that the rate is first order with respect to the substrate. At a given pH, k_{in} was measured in the presence of various concentrations of ZnL (0.4−1.6 mM).[42] The plot of k_{in} vs [total Zn(II) complexes] gave a straight line with the slope denoted as k_{obs}, an example of which is illustrated in Figure 6.

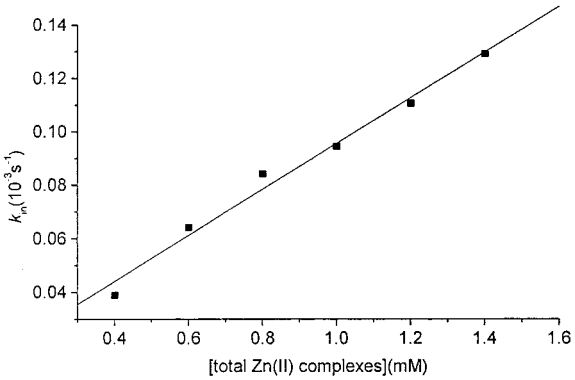

Figure 6. Dependence of k_{in} on [total Zn(II) complexes] at pH 8.09, ionic strength 0.1 M, and at 25 °C in the presence of 10% (v/v) CH_3CN. The slope of the straight line illustrated in the figure is denoted as k_{obs}.

The observed rate constants k_{obs} are 0.12 ± 0.01 M^{-1} s^{-1} at pH 8.90, 0.10 ± 0.01 M^{-1} s^{-1} at pH 8.55, and 0.086 ± 0.01 M^{-1} s^{-1} at pH 8.09 at 25 °C. At these pH values, as shown in the species distribution diagram, the major ingredient of the Zn(II)-containing complexes is the $ZnH_{-1}L$. According to these data, it can be concluded that, as has been testified before, it is the Zn(II)−alkoxide that promotes the cleavage of the carboxy ester bonds.

The second-order rate constant k_{NA} for ZnL of 0.13 ± 0.01 M^{-1} s^{-1}, calculated from k_{obs} with the aid of the deprotonation constants, and other k_{NA} values of NA hydrolysis promoted by several Zn−polyamine ligands complexes are listed in Table 5. It is found that the catalytic efficiency of our ZnL is very much close to Zn−alcohol-pendent [12]aneN_3 complex **III** and much bigger than that of Zn−[12]aneN_3 (**IV**).

^{1}H NMR Studies on the Mechanism of the $ZnH_{-1}L$-Promoted NA Hydrolysis. To elucidate the mechanism of the ZnL-promoted NA hydrolysis, the NA hydrolysis (Scheme 2) was followed by ^{1}H NMR with **I** (10 mM) and NA (10 mM) at pD 8.9 (by NaOD) in nonbuffered 10% (v/v) CD_3CN/D_2O

(42) Suh, J.; Son, S. J.; Suh, M. P. *Inorg. Chem.* **1998**, *37*, 4872.

Table 5. Comparison of Hydrolysis Rate Constants, k_{NA} (M^{-1} s^{-1}), for ZnL, **III**−**VII**, and Aqueous OH^- Ion at $I = 0.1$ ($NaNO_3$) and 25 °C in 10% (v/v) CH_3CN

catal[d]	k_{NA}	catal[d]	k_{NA}
ZnL	0.13 ± 0.01	**III**	0.14[a]
IV	3.6×10^{-2} [a]	**V**	0.10[b]
VI	4.7×10^{-2} [c]	**VII**	0.46[c]
OH^-_{aq}	8.1[b]		

[a] From ref 12. [b] From ref 10. [c] From ref 11. [d] The actual nucleophiles are $ZnH_{-1}L$ for **III**, **VII,** and the present complex and ZnL(OH) for **IV**−**VI**.

Scheme 2

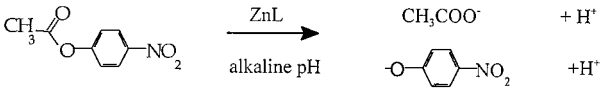

solution at 25 °C at 10, 30, and 60 min. The gradual disappearance of the reactant NA signals (δ 2.38 (CH_3) and 7.40 and 8.34 (ArH)) matched the appearance of the resonances of the product CH_3COO^- (δ 1.90) and 4-nitrophenolate (δ 6.57 and 8.07). No extra peaks were found in the spectra. It is postulated that, in alkaline solution, the transient "acyl intermediate" generated by the attack of Zn(II)-bound alkoxide toward NA seems to be very unstable and disappeared very rapidly at alkaline solution.

To show explicit proton signals of the intermediate, both pH and the concentration of the reactants were reduced to decelerate the intramolecular hydrolysis. ^{1}H NMR study of the NA hydrolysis in nonalkali solution at pD 7.5 showed gradual appearance of new signals (δ 3.65 (CCH_2O), 3.09 (CCH_2NH_2), 2.69 (NCH_2C-acyl pendent)) ca. 3 h after mixing **I** (5 mM) and NA (5 mM) in 20% (v/v) CD_3CN/D_2O solution at 25 °C, which have been assigned respectively to the methylene protons of the transient intermediate (see Figure 7). The gradual appearance of the intermediate resonance signals can be explicated as follows: In the first period of the reaction, acidic reagents (acetic acid and NP) were produced, and with the pH of the solution lowered, the intramolecular hydrolysis was hindered; then the intermediate species accumulated to be explicitly detected by NMR hours later. It is found that, at pH ca. 6 or lower, the intermediate can exit in aqueous solution for long; however, if the pD of the above solution was adjusted again to 8.8 with NaOD, the resonances of the above-mentioned intermediate disappeared quickly. Since the signals of the ZnL complex remained unchanged in the course of the ester hydrolysis, the reaction was testified to be catalytic. These results indicate that, in the course of the catalytic NA hydrolysis promoted by ZnL, the "acyl intermediate" was initially formed as the result of the attack of Zn(II)-bound alkoxide toward NA and then disappeared immediately at alkaline pH to give the final hydrolysis products CH_3COO^- and the starting ZnL complex to complete the catalytic cycle.

Thus, we propose the overall catalytic reaction depicted in Scheme 3, with the initial formation of "acyl intermediate" being the slowest step, which is consistent with the previously proposed "double-hydrolysis" mechanism of the Zn(II)−alcohol-pendent [12]aneN_3.[11,12]

The kinetics of the ZnL-promoted NA hydrolysis shows that Zn(II)-bound alkoxide can be a better nucleophile than a Zn(II)-bound hydroxide, and the present work provides other evidence for the strong nucleophilic attack of Zn(II)-bound alkoxide toward carboxy ester.

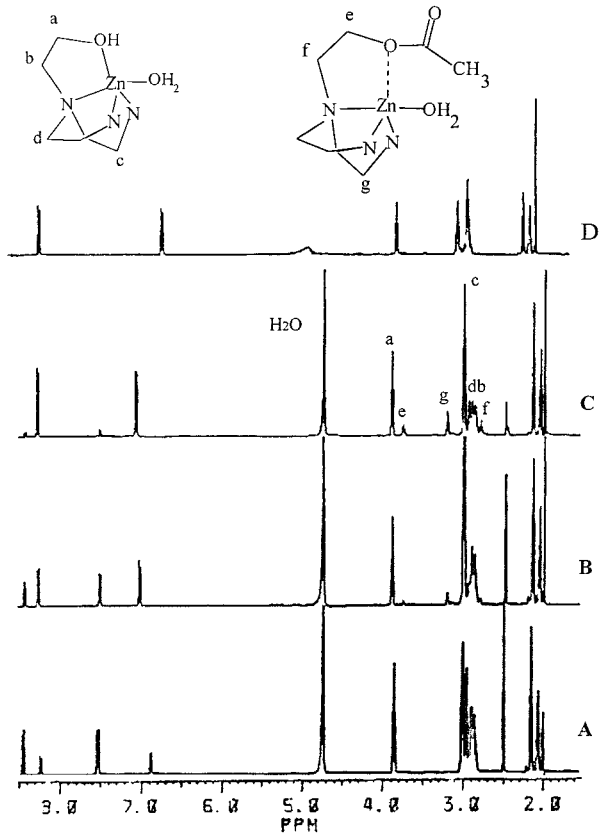

Figure 7. Time-dependent ^{1}H NMR spectra for the 5 mM ZnL/5 mM NA system at 25 °C and 20% (v/v) CD_3CN/D_2O solution. Key (from bottom to top): A, 5 min; B, 4 h; C, 10 h after mixing of NA and **I**; D, soon after pD value of the system is adjusted to 8.8 with NaOD. Peaks assignments: a (t, δ 3.79); b (t, δ 2.79); c (t, δ 2.87); d (t, δ 2.82); e (t, δ 3.65); f (t, δ 2.69); g (t, δ 3.09); NA (t, δ 2.38 (CH_3), 7.40 and 8.34 (ArH)); CH_3COO^- (t, δ 1.90); 4-nitrophenolate (δ 6.96 and 8.19 (pH-dependent)). The peaks in the methyl region (δ 1.96) are due to the impurity in the solvent, which probably concealed the methyl group of the transient "acyl intermediate". By the way, because the complex used is **I**, 33% of which is deprotoned, the signals a−d should be the co-effect of the ZnL and $ZnH_{-1}L$. The assignment of a−d is confirmed by COSY and NOESY spectra.

Scheme 3

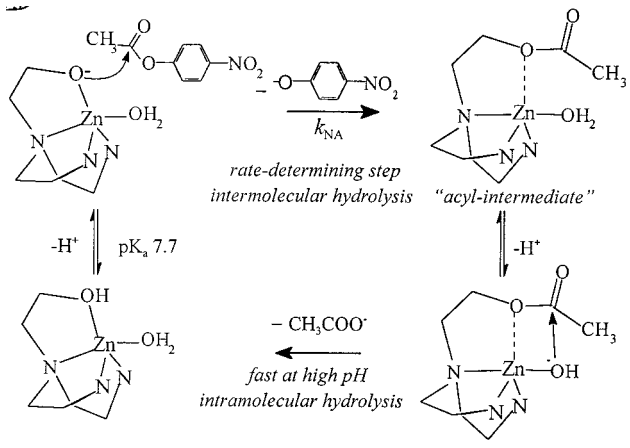

Conclusion

An asymmetric tripodal ligand, 2-[bis(2-aminoethyl)amino]-ethanol, has been chosen to mimic the coordination surrounding and geometry of the Zn(II) cation in alkaline phosphatase. When coordinated to Zn(II), the hydroxyl group of L deprotonates with

a very low pK_a value of 7.7, and then the coordinated water releases the second hydrogen atom with pK_a = 9.8 at 25 °C. X-ray diffraction analysis of the monomeric and dimeric complexes and ES-MS analysis of the aqueous solution provided evidence for the existence of Zn(II)−alkoxide. The 4-nitrophenyl acetate (NA) hydrolysis promoted by the Zn(II)−L complex showed a second-order rate constant of 0.13 M^{-1} s^{-1} and proved that the Zn(II)-bound alkoxide is the reactive nucleopile toward the hydrolysis of esters. Thus, it is first example that tripodal heteropolyamines and their Zn(II) complexes can also be good models for Zn(II)-containing enzymes and are at least as good as macrocyclic polyamines.

Acknowledgment. This work is supported by the National Natural Science Foundation of China. We are thankful to Mr. Jun Hu for his kind help.

Supporting Information Available: X-ray data in CIF format. This material is available free of charge via the Internet at http://pubs.acs.org.

IC000642N